

Note

Metal-directed 1-D molecular-box based coordination polymers with mono- and di-nuclear nodes – Construction of 3-D supramolecular networks via hydrogen bonding and S··S interactions

Miao Du *, Cheng-Peng Li

College of Chemistry and Life Science, Tianjin Normal University, 241, Wei Jin Road, Tianjin 300074, PR China

Received 4 September 2005; received in revised form 11 November 2005; accepted 23 November 2005

Available online 10 January 2006

Abstract

Self-assemblies of 4-pyridylthioacetic acid (Hpyta) with CdCl₂ or HgCl₂ yield the polymeric metal-organic coordination frameworks [Cd(pyta)₂(H₂O)]_n (**1**) and [Hg(pyta)Cl]_n (**2**). X-ray single-crystal diffraction results reveal that both complexes display similar 1-D neutral coordination arrays containing approximate rectangular molecular box subunits, which are, however, linked via mononuclear Cd^{II} and dinuclear Hg₂O₂ nodes. For **1**, the adjacent 1-D motifs are interconnected to form a 2-D layer via O–H···O hydrogen bonds and further engender a 3-D network by weak S··S interactions; whereas complex **2** possesses a novel 3-D supramolecular architecture with the aid of abundant C–H···Cl and S··S contacts. Interestingly, due to the intrinsic difference of the metal ions, the carboxylate group of the pyta ligand displays symmetric bidentate chelate mode for **1** and monoatomic bridging fashion for **2**; the latter case is unprecedented in coordination chemistry of pyta. These results clearly suggest that it is an effective synthetic strategy by employing coordinative forces and concomitant noncovalent contacts to construct the fine-tuning supramolecular networks.

© 2005 Elsevier B.V. All rights reserved.

Keywords: Crystal engineering; 4-Pyridylthioacetate; Supramolecular assembly; Coordination polymer; Hydrogen bond and S··S interaction

1. Introduction

One of the fascinating themes of current chemistry is crystal engineering of metal-organic coordination frameworks, which usually display interesting network structures and desired properties [1–5]. So far, several efficient strategies have been developed for design and creation of such inorganic–organic hybrid materials, which would essentially meet the requirement of ligand function and metal coordination tendency, as well as energetic considerations of the whole supramolecular system [6–8]. Beyond the robust metal–ligand coordination, other noncovalent forces have also been proven to be powerful tools to fabricate fine-tuning functional architectures [9]. These weak

secondary interactions [10–12], such as hydrogen bonds, π – π stacking and van der Waals forces, make the molecular assembly reversible and variable, and as a consequence, provide synthetic flexibility and functional diversity.

In this direction, we are interested in utilizing the interplay of such interactions to create new crystalline coordination solids with versatile building blocks. Recently, we have investigated the supramolecular assemblies of a variety of metal ions with the flexible ligands 4-pyridylacetic acid (Hpya) and 4-pyridylthioacetic acid (Hpyta), which possess –CH₂– and longer –SCH₂– spacers between the pyridyl and carboxyl groups, respectively, as well as different spatial tropisms [13,14]. Comparatively, the longer Hpyta ligand is more attractive in the aspects of adjustable configuration (see Chart 1) and binding modes, and a potential site for weak S··S interactions, which will facilitate the formation of peculiar networks. In this context, we will describe here the construction of two new metal-organic frameworks

* Corresponding author. Tel.: +86 22 2354 0315/2353 8221; fax: +86 22 2354 0315.

E-mail address: dumiao@public.tpt.tj.cn (M. Du).

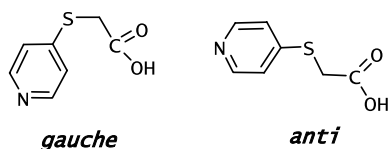


Chart 1.

through assembly of Hpyta and the d^{10} Cd^{II} / Hg^{II} metal ions, that is, $[\text{Cd}(\text{pyta})_2(\text{H}_2\text{O})]_n$ (**1**) and $[\text{Hg}(\text{pyta})\text{Cl}]_n$ (**2**). In both cases, the 1-D arrays are extended to result in 3-D supramolecular architectures through concomitant hydrogen bonding and $\text{S} \cdots \text{S}$ interactions, which are rare in metal–pyta chemistry. Notably, a new binding mode of pyta [$\mu_3, \eta^2(\text{N}_{\text{py}}, \mu\text{-O}, \text{O}_{\text{COO}^-})$] was observed in the Hg^{II} complex.

2. Experimental

2.1. Materials and general methods

All the reagents were commercially available and used without further purification. Distilled water was used throughout. Fourier transform (FT) IR spectra (KBr pellets) were taken on an AVATAR-370 (Nicolet) spectrometer. Elemental (C, H and N) analyses were performed on a CE-440 (Leemanlabs) analyzer.

2.2. Syntheses of the complexes **1** and **2**

$[\text{Cd}(\text{pyta})_2(\text{H}_2\text{O})]_n$ (**1**). The pH value of a hot aqueous solution (5 mL) of Hpyta (17 mg, 0.1 mmol) was adjusted to ca. 6 by dropwise addition of an aqueous solution of KOH (0.1 M), which was placed in a straight glass tube. A solution of $\text{CdCl}_2 \cdot 2.5\text{H}_2\text{O}$ (23 mg, 0.1 mmol) in MeOH (5 mL) was then carefully layered onto it. Upon slow evaporation of the solvents, prismatic colorless single crystals suitable for X-ray analysis were obtained after 3 days in 65% yield (based on Hpyta). IR (KBr, cm^{-1}): 3381b, 2911s, 1588vs, 1483s, 1413vs, 1229s, 1169s, 1110m, 1072w, 1014m, 935w, 904w, 807s, 700s, 496s. *Anal.* Calc. for $\text{C}_{14}\text{H}_{14}\text{CdN}_2\text{O}_5\text{S}_2$: C, 45.79; H, 4.39; N, 7.63. Found: C, 45.82; H, 4.54; N, 7.34%.

$[\text{Hg}(\text{pyta})\text{Cl}]_n$ (**2**). The same synthetic procedure as for **1** was used except that the metal salt was replaced by HgCl_2 (27 mg, 0.1 mmol), producing colorless block single crystals by slow evaporation of the solvents after a period of 2 weeks in 53% yield. IR (KBr, cm^{-1}): 1596vs, 1481s, 1426m, 1385w, 1349vs, 1221m, 1117m, 1062s, 1028w, 902w, 866w, 814s, 775w, 731m, 703w, 574w, 494m, 420w. *Anal.* Calc. for $\text{C}_7\text{H}_6\text{ClHgNO}_2\text{S}$: C, 22.59; H, 1.62; N, 3.76. Found: C, 22.77; H, 1.35; N, 3.84%.

2.3. X-ray crystallographic data collection and structural determination

X-ray single-crystal diffraction data for **1** and **2** were collected on a Bruker Apex II CCD diffractometer at 293(2) K

Table 1

Crystallographic data and structure refinement summary for complexes **1** and **2**

	$\text{C}_{14}\text{H}_{14}\text{CdN}_2\text{O}_5\text{S}_2$	$\text{C}_7\text{H}_6\text{ClHgNO}_2\text{S}$
Formula	$\text{C}_{14}\text{H}_{14}\text{CdN}_2\text{O}_5\text{S}_2$	$\text{C}_7\text{H}_6\text{ClHgNO}_2\text{S}$
Molecular weight	466.79	404.23
Crystal system	monoclinic	triclinic
Crystal size (mm)	$0.48 \times 0.06 \times 0.04$	$0.22 \times 0.16 \times 0.10$
Space group	$C2/c$	$P\bar{1}$
a (Å)	21.659(6)	7.4853(8)
b (Å)	6.5852(17)	8.4363(9)
c (Å)	15.644(4)	8.5159(9)
α (°)	90	68.7570(10)
β (°)	132.798(3)	75.8410(10)
γ (°)	90	72.1690(10)
V (Å ³)	1637.2(7)	471.70(9)
Z	4	2
D_{calc} (g cm^{-3})	1.894	2.846
μ (mm^{-1})	1.616	16.781
$F(000)$	928	368
2θ -Range for data collection	2.56–25.03	2.60–25.02
Reflections collected	4301	2577
Independent/observed reflections	1449/1163	1637/1448
Range of h, k, l	–25/25, –7/7, –18/18	–8/5, –10/8, –10/10
Parameters	110	118
R_{int}	0.0531	0.0323
R indices ($I > 2\sigma(I)$)	0.0346, 0.0647	0.0365, 0.0905
R indices (all data)	0.0521, 0.0691	0.0433, 0.0947
Goodness-of-fit on F^2	1.056	1.031
Largest difference peak and hole (e Å^{-3})	0.467 and –0.573	2.243 and –2.849

with Mo $\text{K}\alpha$ radiation ($\lambda = 0.71073$ Å) by ω scan mode. There was no evidence of crystal decay during the data collection. Semi-empirical absorption corrections were applied using SADABS program. The program SAINT was used for integration of the diffraction profiles [15]. Both structures were solved by direct methods using the SHELXS program of the SHELXTL package and refined with SHELXL [16]. The final refinement was performed by full-matrix least-squares methods on F^2 with anisotropic thermal parameters for all non-H atoms. C-bound H atoms were placed at calculated positions, with C–H distances of 0.93 and 0.97 Å for aromatic and methene groups, and refined as riding atoms. Starting positions for water hydrogens were located in difference Fourier syntheses; refinement proceeded using a riding model. Isotropic displacement parameters of hydrogen atoms were derived from the parent atoms [$U_{\text{iso}}(\text{H}) = 1.2U_{\text{eq}}(\text{C})$ and $1.5U_{\text{eq}}(\text{O})$]. Further details for crystallographic data and refinement conditions are listed in Table 1.

3. Results and discussion

3.1. Preparation and general characterization of **1** and **2**

In our previous work [14], the crystallization of coordination polymers is performed by direct mixing of Hpyta with a given metal salt, such as Co^{II} , Cu^{II} , Ag^{I} , Zn^{II} , Mn^{II} and Pb^{II} , affording suitable single crystals for X-ray

diffraction; whereas in this study, well-shaped crystals of **1** and **2** were achieved applying the diffusion method. Both complexes display similar neutral 1-D coordination frameworks, however, they have different metal–ligand compositions (1:2 for **1** and 1:1 for **2**), which notably, are independent of the ratio of the starting reagents. The results of elemental analyses were in good agreement with the theoretical requirements of the compositions. In the IR spectra of Hpyta and both complexes, the absorption bands resulting from the skeletal vibrations of the pyridyl groups appear in the 1400–1600 cm^{-1} region. For Hpyta and **1**, the broad band centered at ca. 3400 cm^{-1} suggests the O–H stretching of carboxyl or aqua ligand. The IR spectrum of Hpyta shows the characteristic absorption bands of –COOH in 1693 and 1483 cm^{-1} . For **1** and **2**, the peaks at 1588 and 1596 cm^{-1} attribute to the antisymmetric stretching vibrations, as well as 1413 and 1349 cm^{-1} to the symmetric vibrations of the carboxylate groups. The Δ parameter ($\nu_{\text{as}} - \nu_{\text{sym}}$) of **2** (247 cm^{-1}) is larger than that of **1** (175 cm^{-1}), which agrees with their solid structural features (monoatomic bridging or symmetric bidentate chelated coordination mode) [17].

3.2. Structural analysis

$[\text{Cd}(\text{pyta})_2(\text{H}_2\text{O})]_n$ (**1**). Complex **1** has a 1-D infinite coordination framework, as shown in Fig. 1A, in which the Cd^{II} center is connected to two pyridyl nitrogen atoms, one aqua ligand and four oxygens from a pair of carboxylates adopting the symmetric bidentate chelate mode ($\eta\text{-O}_2\text{O}'$). Thus, the local coordination environment around the Cd^{II} center (CdN_2O_5) can be properly portrayed as a slightly distorted pentagonal bipyramid (see Fig. 1A caption for detailed bond geometries). The Cd^{II} atom ideally locates at the pentagonal basal plane defined by O1B–O2B–O3–O2C–O1C, with the axial positions being occupied by two pyridyl nitrogens. Two C–O bond lengths of each carboxylate group are nearly equivalent, being consistent with its binding fashion. The pyta anionic ligand adopts the *gauche* configuration, which is approved by the C5–S1–C6–C7 torsion angle [$-68.2(3)^\circ$] between the central C–S bond, and pyridyl and carboxylate groups. A pair of centrosymmetric *gauche*-pyta links the adjacent Cd^{II} centers to generate a tetragonal molecular-box unit with the size of ca. $5.35 \times 6.85 \text{ \AA}^2$, and these subunits are extended to a 1-D coordination framework along the crystallographic [001] direction. Within each dimeric subunit, the neighboring $\text{Cd} \cdots \text{Cd}$ separation is 8.749(2) Å , and the center-to-plane distance is 3.871 Å for two antiparallel pyridyl rings, however, without any overlap.

Further analysis of the crystal packing of **1** indicates that the noncovalent interactions also play a vital role. As shown in Fig. 1B, each coordinated water forms a pair of O3–H3A \cdots O1 i ($i = x, -y + 1, z + 1/2$) hydrogen bonds with the carboxylate oxygens in the neighboring 1-D array with the formation of a $R_2^2(6)$ pattern [18]. The H \cdots O and O \cdots O separations are 1.986 and 2.756 Å , respectively, and

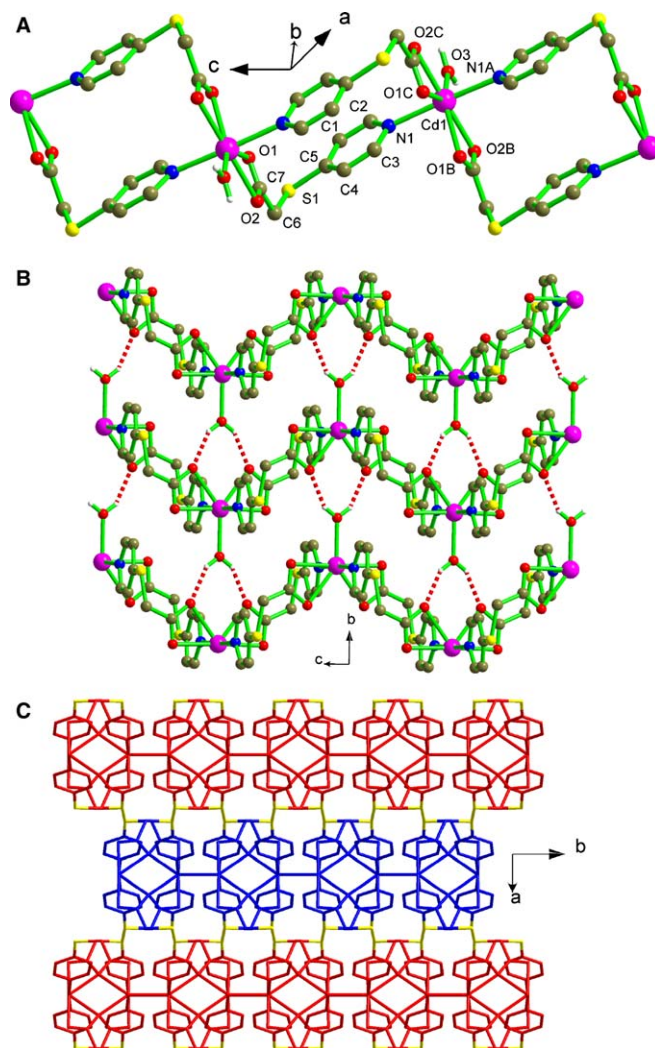


Fig. 1. (A) 1-D framework of **1** with atom labeling of the asymmetric unit and Cd^{II} coordination sphere (symmetry operations A: $-x, y, -z + 1/2$; B: $x, -y + 2, z + 1/2$; C: $-x, -y + 2, -z$). Key geometric parameters: Cd1–N1 2.322(3), Cd1–O2B 2.385(3), Cd1–O1B 2.461(3), Cd1–O3 2.319(4), C7–O1 1.248(5), C7–O2 1.245(5) Å ; O3–Cd1–N1 92.36(9), N1A–Cd1–N1 175.27(18), N1–Cd1–O2C 89.84(11), O2B–Cd1–O2C 177.91(14), O3–Cd1–O2B 88.96(7), N1–Cd1–O2B 90.24(11), N1–Cd1–O1C 88.43(11), O2C–Cd1–O1B 128.53(10), O2B–Cd1–O1B 53.56(9), O3–Cd1–O1B 142.51(7), O1B–Cd1–O1C 74.98(14), N1–Cd1–O1B 87.81(12) $^\circ$. (B) A perspective of the 2-D hydrogen-bonded layer via interchain O–H \cdots O interactions. (C) 3-D supramolecular architecture via interlayer S \cdots S weak interactions, which are highlighted in yellow between the adjacent layers marked in red and blue. (For interpretation of the references to color in this figure legend, the reader is referred to the web version of this article.)

the O–H \cdots O bond angle is 149 $^\circ$, falling into the normal range of such forces. As a consequence, these inter-chain hydrogen bonds connect the 1-D frameworks to result in a 2-D network along the (011) plane. It is noteworthy to point that, aside from the hydrogen bonds, the interlayer S \cdots S interaction is another useful organizing force in this supramolecular assembly. The nearest non-bonding S \cdots S distance between two adjacent layers is 3.579 Å , being shorter than the van der Waals S–S contact distance [14]. Thus, such weak interactions extend the 2-D parallel

layers, which closely arrange in an SS/SS' sequence with approximate offset of $0.5b$, into a 3-D supramolecular architecture as shown in Fig. 1C.

$[Hg(pyta)Cl]_n$ (2). X-ray single-crystal determination of 2 also reveals a similar neutral 1-D polymeric motif. As depicted in Fig. 2A, the local environment around each Hg^{II} center gives rise to a distorted tetrahedral geometry, and is attached by one pyridyl nitrogen, two carboxylate oxygens from distinct pyta ligands and a charge-assisted chloride ion (see Fig. 2A caption for detailed bond parameters). As expected, the bond length of O1–C7 is longer than that of O2–C7. In the same way, the pyta ligand adopts the *gauche* configuration, reflected by the C5–S1–C6–C7 torsion angle of $70.6(8)^\circ$. Interestingly, each carboxylate group of pyta behaves as a μ -O,O bridging coordination mode, which is unprecedented in metal–pyta complexes (see detailed discussion below). As a consequence, the Hg^{II} ions are connected by the bridging pyta ligands to form a 1-D molecular-box based coordination framework along the [100] direction, as shown in Fig. 2B, which is similar to 1, however, has dimeric Hg_2O_2 subunits as the nodes. Within each dinuclear node, the Hg–O–Hg bridging angle is $114.4(2)^\circ$ and the Hg \cdots Hg distance is 4.264(1) Å. In the dimeric box-like $[Hg(pyta)]_2$ unit with the size of ca. $5.55 \times 6.65 \text{ \AA}^2$, the separation of the diagonal Hg \cdots Hg linked through a *gauche*-pyta is 8.801(3) Å, and the center-to-plane distance is 3.813 Å for two antiparallel pyridyl rings, also without any overlap as in 1.

An intrachain C3–H3 \cdots Clⁱ ($i = -x, 1 - y, -z$) interaction between the 2-position C–H group of the pyridyl ring and chloride ligand is observed (H \cdots Cl/C \cdots Cl distances: 2.857/3.663 Å; C–H \cdots Cl angle: 146°). As illustrated in Fig. 2C, further self-assembly by means of interchain C2–H2 \cdots Clⁱⁱ ($ii = -x, -y, -z$) contacts (H \cdots Cl/C \cdots Cl distances: 2.872/3.663 Å; C–H \cdots Cl angle: 144°) of the adjacent 1-D arrays affords a 2-D hydrogen-bonded layer along the crystallographic (1 10) plane. Additionally, these parallel 2-D layers are combined into the final 3-D supramolecular network [see Fig. 2D] through interlayer C6–H6 \cdots Clⁱⁱⁱ ($iii = 1 + x, 1 + y, z$) hydrogen bonds (H \cdots Cl/C \cdots Cl distances: 2.870/3.640 Å; C–H \cdots Cl angle: 137°), as well as weak S \cdots S interactions (S \cdots S = 3.485 Å). All hydrogen bond geometries lie in the normal range [11,19].

It is notable to point out that the versatile C–H \cdots Cl–M weak interactions have been shown to be capable of playing the crucial role in the structure building of supramolecular complexes [19,20]. In the present case of 2, from the viewpoint of charge distribution in the pyridyl ring of pyta, with the electron shifting from the ring carbon atoms toward nitrogen, as well as the contribution of electron density to the metal ion, the α -pyridyl carbon atoms are electron deficient and such C–H groups are more apt to participate in sp^2 -C–H \cdots Cl–M contacts [19]. Meanwhile since the electron affinity of the carboxylate and pyridylthio groups is toward the $-\text{CH}_2-$ spacer in pyta, its H atoms are acidic and tempted to be involved in sp^3 -C–

H \cdots Cl–M interactions. As a consequence, each chloride ion acts as the hydrogen acceptor to trifurcated pyta moieties, and such noncovalent forces, together with weak S \cdots S interactions, are well organized to tailor the whole supramolecular structure.

3.3. A summary of coordination fashions of pyta

It could be concluded that pyta has a strong ability to directly construct a variety of metal-organic coordination frameworks with most of the common metal ions such as Mn^{II} [14,29,30], Co^{II} [14,28], Ni^{II} [21,25,26], Cu^{II} [14,22,23], Zn^{II} [14,24,27], Cd^{II} , Hg^{II} , Ag^I [14,28] and Pb^{II} [14], which, undoubtedly, should attribute to its structural flexibility and versatile coordination modes (sometimes even in two ways within a structure). Several synthetic approaches have been successfully applied to realize the metal–pyta coordination compounds, such as solvent evaporation [14,23,28], hydrothermal synthesis [21,22,25–30], and diffusion method [24, this work]. Notably, several possible coordination motifs may be achieved under different conditions in the assembly of Hpyta with a given metal ion. For example, a 1-D box-like, a 2-D square-grid and a 2-D homo-chiral helical Zn^{II} coordination polymer of pyta have been reported so far. A summary and comparison of the binding fashions of pyta in the known structures (see Chart 2 for details) may be helpful to understand the assembly processes and further rational design of new coordination solids in future. The following two notable features of pyta chemistry should be emphasized. Firstly, the configuration of pyta is always *gauche*, and only four cases of *anti*-pyta complexes with similar mononuclear structures are obtained, in which the carboxylate group is free of binding to the metal ion [14,21–23]. Remarkably, both configurations are detected in a unique $\{[Zn(pyta)_2] \cdot 4H_2O\}_n$ complex [14]. Secondly, there are three potential coordination functional groups such as pyridyl, carboxylate and thioether in pyta, which exhibit different coordination tendencies to metal ions. The pyridyl nitrogen is bound to the metal center in all the cases. Only in the 2-D silver-pyta network, the thioether moiety is active in the formation of coordination framework. As expected, a variety of coordination modes of carboxylate are found in the pertinent structures (Chart 2), including monodentate (I) [14,24–26], symmetric bidentate chelate (II) [25,26,28–30, this work], asymmetric bidentate chelate (III) [14,27], μ -O,O (IV) [this work] and *syn-anti* bridging (V) [14,28] fashions. Generally speaking, the nature of the metal center has a significant influence on the ligand coordination modes. In this context, the carboxylate group of pyta adopts the binding mode II for Mn^{II} [29,30] and Cd^{II} [this work], V for Ag^I [14,28], IV for Hg^{II} [this work] and III for Pb^{II} [14]. Of further interest, the carboxylate moiety may display a variety of binding styles with respect to the same metal ion, such as uncoordinated [14] and mode II [28] for Co^{II} ; uncoordinated [21] and simultaneous I/II [25,26] for Ni^{II} ; uncoordinated [22,23] and simultaneous

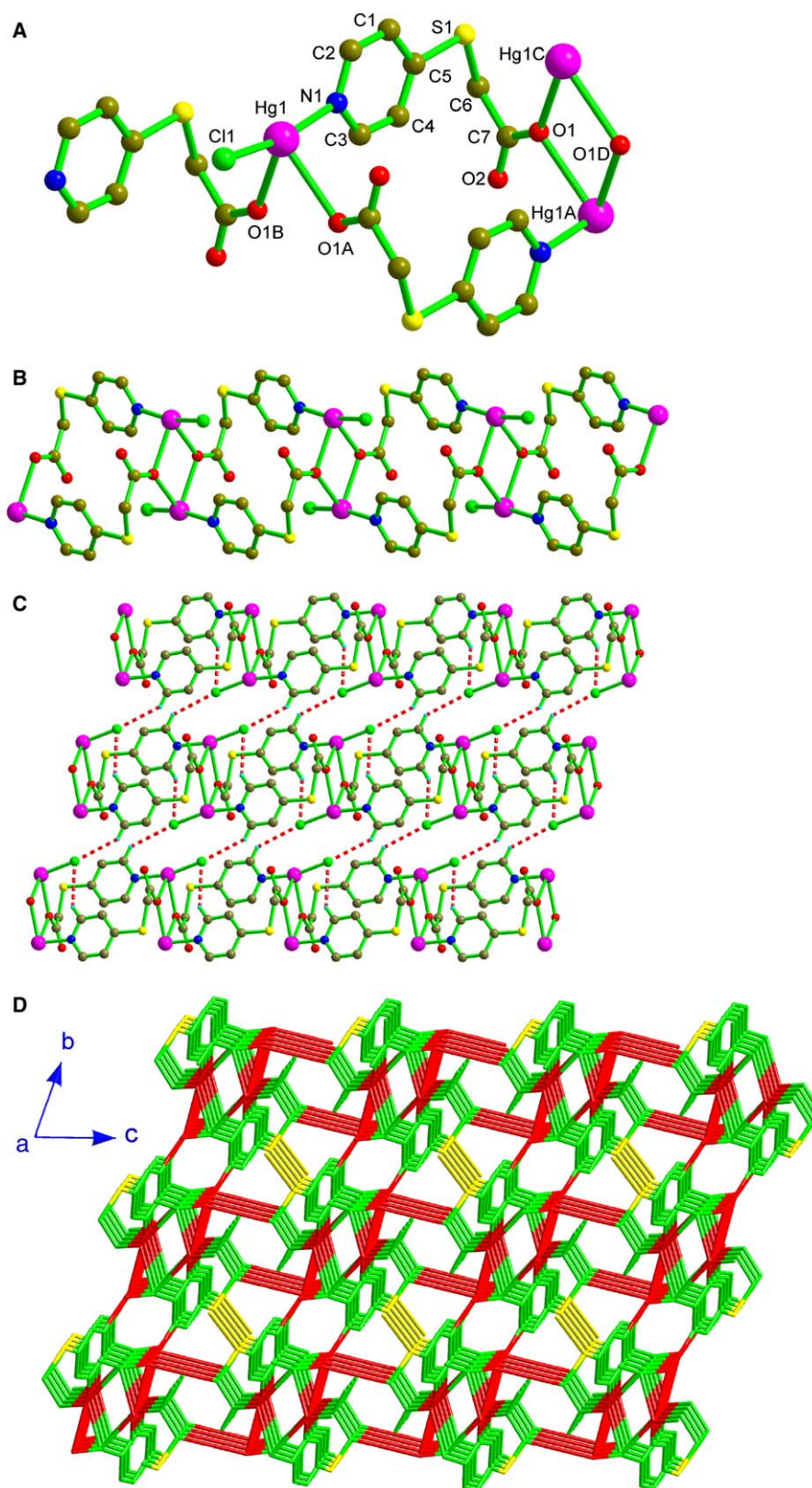


Fig. 2. (A) A portion view of **2** with atom labeling of the asymmetric unit, as well as the Hg^{II} coordination sphere and binding mode of carboxylate (symmetry operations A: $-x + 1, -y + 1, -z$; B: $x - 1, y, z$; C: $x + 1, y, z$; D: $-x + 2, -y + 1, -z$). Key geometric parameters: Hg1–N1 2.139(8), Hg1–Cl1 2.323(3), Hg1–O1A 2.510(6), Hg1–O1B 2.562(7), O1–C7 1.238(11), O2–C7 1.218(13) Å; N1–Hg1–Cl1 165.8(2), N1–Hg1–O1A 91.3(3), Cl1–Hg1–O1A 97.64(18), N1–Hg1–O1B 89.8(3), Cl1–Hg1–O1B 103.85(13), O1A–Hg1–O1B 65.6(2)°. (B) 1-D box-like coordination motif with dimeric nodes along the crystallographic [100] direction. (C) 2-D hydrogen-bonded array along *ab* plane via C–H···Cl forces. (D) View of the 3-D supramolecular network via weak C–H···Cl and S···S interactions, which are highlighted in red and yellow, respectively. (For interpretation of the references to color in this figure legend, the reader is referred to the web version of this article.)

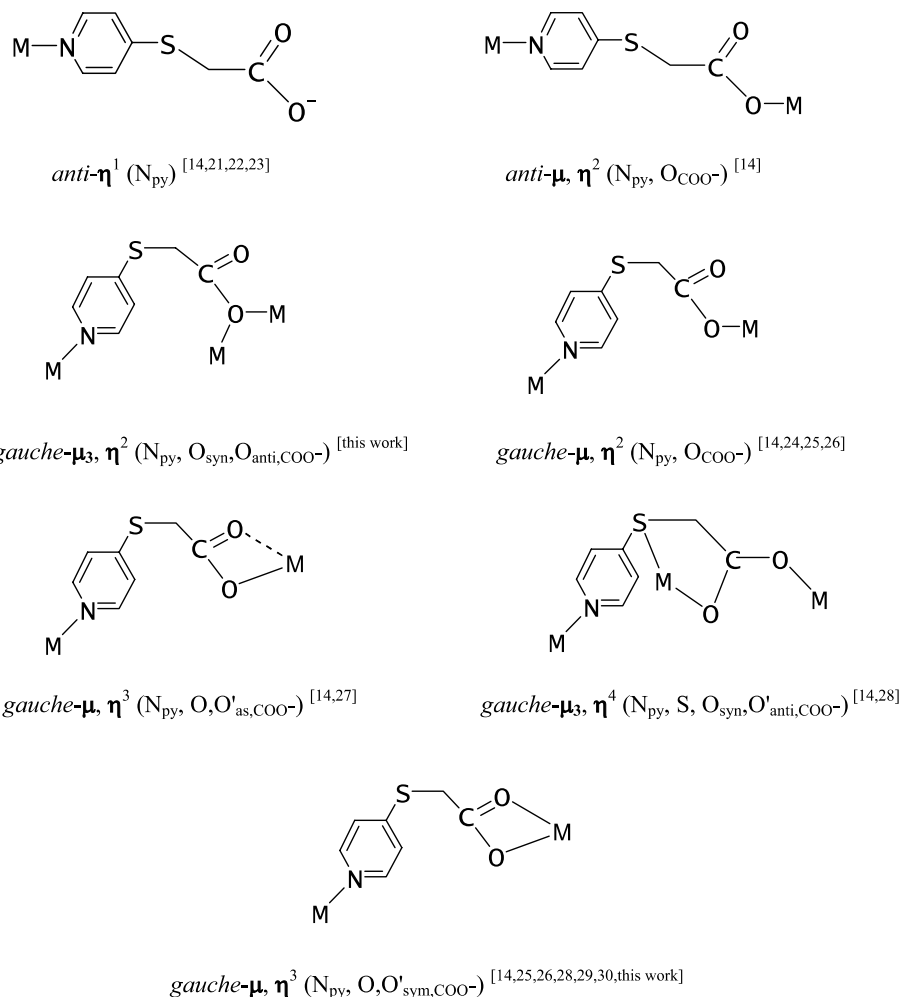


Chart 2.

I/III [14] for Cu^{II}; and I [24], III [27] and simultaneous I/III [14] for Zn^{II}.

In conclusion, a versatile flexible ligand Hpyta has been successfully employed to achieve its *first* Cd^{II} and Hg^{II} coordination polymers [Cd(pyta)₂(H₂O)]_n (**1**) and [Hg(pyta)Cl]_n (**2**). The presence of novel supramolecular networks of **1** and **2** is mainly due to the diverse coordination fashions and strong capability to create complicated weak interactions of pyta. For both cases, the 1-D molecular-box based metal-organic frameworks with mono- and di-nuclear nodes, directed only by the selection of metal ions, are extended to 3-D architectures through additional hydrogen bonds and weak S··S interactions. Anyway, this synthetic strategy by combining the strong coordination bonds and weak noncovalent interactions may further enrich the crystal engineering of metal-organic supramolecular solids.

Acknowledgments

The authors gratefully acknowledge the financial support from the National Natural Science Foundation of China (No. 20401012), the Key Project of Tianjin Natural Science Foundation (No. 043804111) and Tianjin Normal University (to M. Du).

Appendix A. Supplementary data

Crystallographic data (excluding structure factors) for the crystal structures reported in this paper have been deposited with the Cambridge Crystallographic Data Center (CCDC Nos. 2822 47/48). This material can be obtained free of charge via www.ccdc.cam.ac.uk/conts/retrieving.html (or from the CCDC, 12 Union Road, Cambridge CB2 1EZ, UK; fax: +44 1223 336 033; e-mail: deposit@ccdc.cam.ac.uk). Supplementary data associated with this article can be found, in the online version, at [doi:10.1016/j.ica.2005.11.038](https://doi.org/10.1016/j.ica.2005.11.038).

References

- [1] O.M. Yaghi, H. Li, C. Davis, D. Richardson, T.L. Groy, *Acc. Chem. Res.* 31 (1998) 474.
- [2] B. Moulton, M.J. Zaworotko, *Chem. Rev.* 101 (2001) 1629.
- [3] W. Lin, O.R. Evans, *Acc. Chem. Res.* 35 (2002) 511.
- [4] S.R. Batten, K.S. Murray, *Coord. Chem. Rev.* 246 (2003) 103.
- [5] D. Bradshaw, J.B. Claridge, E.J. Cussen, T.J. Prior, M.J. Rosseinsky, *Acc. Chem. Res.* 38 (2005) 273.
- [6] R. Robson, *J. Chem. Soc., Dalton Trans.* (2000) 3735.
- [7] C. Janiak, *Dalton Trans.* (2003) 2781.
- [8] G.R. Desiraju, *J. Mol. Struct.* 656 (2003) 5.

- [9] M.W. Hosseini, *Acc. Chem. Res.* 38 (2005) 313.
- [10] C. Janiak, *J. Chem. Soc., Dalton Trans.* (2000) 3885.
- [11] G.R. Desiraju, T. Steiner, *The Weak Hydrogen Bond in Structural Chemistry and Biology*, Oxford University Press, Oxford, 1999.
- [12] M. Nishio, *CrystEngComm* 6 (2004) 130.
- [13] M. Du, C.-P. Li, X.-J. Zhao, *Cryst. Growth Des.* 6 (2006) 335.
- [14] M. Du, X.-J. Zhao, Y. Wang, *Dalton Trans.* (2004) 2065.
- [15] Bruker AXS, *SAINT Software Reference Manual*, Madison, WI, 1998.
- [16] G.M. Sheldrick, *SHELXTL NT Version 5.1. Program for Solution and Refinement of Crystal Structures*, University of Göttingen, Germany, 1997.
- [17] K. Nakamoto, *Infrared and Raman Spectra of Inorganic and Coordination Compounds*, Wiley, New York, 1986.
- [18] The graph set topological terminology for the analysis of hydrogen-bonded patterns is described in: M.C. Etter, *Acc. Chem. Res.* 23 (1990) 120.
- [19] V. Balamurugan, M.S. Hundal, R. Mukherjee, *Chem. Eur. J.* 10 (2004) 1683.
- [20] P.K. Thallapally, A. Nangia, *CrystEngComm* 3 (2001) 114.
- [21] X.M. Zhang, R.Q. Fang, H.S. Wu, S.W. Ng, *Acta Crystallogr., Sect. E* 60 (2004) m135.
- [22] R.Q. Fang, X.M. Zhang, H.S. Wu, S.W. Ng, *Acta Crystallogr., Sect. E* 60 (2004) m401.
- [23] Y.Q. Huang, H. Zhang, J.G. Chen, W. Zou, L. Li, Z.B. Wei, S.W. Ng, *Acta Crystallogr., Sect. E* 60 (2004) m133.
- [24] M. Kondo, M. Miyazawa, Y. Irie, R. Shinagawa, T. Horiba, A. Nakamura, T. Naito, K. Maeda, S. Utsuno, *F. Uchida, Chem. Commun.* (2002) 2156.
- [25] Y.Q. Huang, H. Zhang, J.G. Chen, W. Zou, S.W. Ng, *Acta Crystallogr., Sect. E* 60 (2004) m935.
- [26] Y.Q. Huang, H. Zhang, J.G. Chen, W. Zou, S.W. Ng, *Acta Crystallogr., Sect. E* 60 (2004) m933.
- [27] X.M. Zhang, R.Q. Fang, H.S. Wu, S.W. Ng, *Acta Crystallogr., Sect. E* 59 (2003) m1194.
- [28] S.B. Qin, Y.X. Ke, S.M. Lu, J.M. Li, H.X. Pei, X.T. Wu, W.X. Du, *J. Mol. Struct.* 689 (2004) 75.
- [29] Y.Q. Huang, H. Zhang, J.G. Chen, S.W. Ng, *Acta Crystallogr., Sect. E* 60 (2004) m1051.
- [30] X.M. Zhang, R.Q. Fang, H.S. Wu, S.W. Ng, *Acta Crystallogr., Sect. E* 60 (2004) m169.